Environment Protection Engineering

Vol. 26 2000 No. 1–2

GORAN T. VLADISAVLEVIĆ*, MILOŠ B. RAJKOVIĆ*

USE OF POLSULFONE HOLLOW FIBERS FOR BUBBLELESS MEMBRANE AERATION OF WATER

Aeration of water with pure oxygen stream was investigated in a bubbleless membrane-based contactor made from 1058 hydrophilic polysulfone hollow fibers. The gauge pressure of 2–4 kPa was maintained in the gas stream in order to prevent fiber leakage. The dissolved oxygen concentration in the outlet water stream decreases with increasing water flow rate and is independent of gas flow rate. At the same water flow rate, the dissolved oxygen concentrations in the product water are much higher for the water flow inside the hollow fibers than those for the water flow outside them. The overall mass transfer coefficient K_L increases with increasing the water flow rate and reaches a constant value at a sufficiently high water flow rate, corresponding to the conditions under which microporous membrane walls control the overall mass transfer.

LIST OF SYMBOLS

A – interfacial contact area, m^2
C – concentration of dissolved oxygen in liquid phase, $kmol \cdot m^{-3}$
C_G – concentration of dissolved oxygen in gaseous phase, $kmol \cdot m^{-3}$
ΔC_m – logarithmic mean driving force for oxygen transfer, $kmol \cdot m^{-3}$
D – diffusion coefficient of dissolved gas in membrane pores, $m^2 \cdot s^{-1}$
d_o – outside diameter of hollow fibers, m
H – Henry's law constant
H' – Yang–Cussler constant, $Q_L/(Q_G H)$
J – permeation oxygen flux, $kmol \cdot m^{-2} \cdot s^{-1}$
k_G – gas film mass transfer coefficient, $m \cdot s^{-1}$
k_L – liquid film mass transfer coefficient, $m \cdot s^{-1}$
k_M – membrane mass transfer coefficient, $m \cdot s^{-1}$
K_L – overall mass transfer coefficient based on liquid phase, $m \cdot s^{-1}$
n_1 – number of hollow fibers in a sheet
Q_G – volumetric flow rate of gas, $m^3 \cdot s^{-1}$
Q_L – volumetric flow rate of liquid, $m^3 \cdot s^{-1}$
Re – Reynolds number
Sc – Schmidt number, $\mu/(\rho D)$

*Institute of Food Technology and Biochemistry, Faculty of Agriculture, University of Belgrade, P.O. Box 127, 11081 Belgrade-Zemun, Yugoslavia. E-mail: gtvladis@afrodita.rcub.bg.ac.yu.

Sh – Sherwood number
v_L – liquid velocity, $m \cdot s^{-1}$
v_G – gas velocity, $m \cdot s^{-1}$
δ – membrane thickness, m
ε – porosity of membrane wall
μ – dynamic viscosity of liquid, Pa·s
ρ – density of liquid, $kg \cdot m^{-3}$
τ – tortuosity of membrane wall

SUPERSCRIPTS

$*$ – denotes the value C in equilibrium with the gas phase concentration C_g
i – denotes oxygen concentrations at the inner membrane surface
o – denotes oxygen concentrations at the outer membrane surface

SUBSCRIPTS

0 – denotes inlet value of C
1 – denotes outlet value of C

1. INTRODUCTION

Membrane-based contactors are devices made from hollow fiber membranes used to effect non-dispersive contacting of two immiscible phases (liquid–liquid or gas–liquid). The advantages of membrane-based contactors over conventional dispersion-phase contactors such as packed towers, spray towers or bubble columns are much larger interfacial areas per unit volume, the constant interfacial area in the entire operating range of flow rates, and the independent control of phase flow rates without flooding or loading problems [1].

The membrane-based gas absorption or stripping may find numerous applications in environmental engineering, such as aeration of water in rivers and wastewater treatment plants [2]–[3], removal of CO_2 and/or SO_2 from flue gases [4]–[9], biological waste gas treatment [10], and removal of volatile organic compounds (VOCs) from water [11]–[14]. Other applications may be itemized as follows: bubbleless aeration of shear-sensitive cell cultures [15], aeration of bioreactors at high oxygen demand [16], blood oxygenation in artificial lungs [17], removal of dissolved oxygen in ultrapure water production [18], gas exchange in artificial gills [19], [20], etc. Two types of gas permeable membranes are used for membrane-based gas absorption processes, i.e. nonporous silicone rubber membranes [8], [9] and microporous membranes made from such glassy polymers as polypropylene [2]–[7], [10]–[20]. Microporous membranes have the advantage of providing very high gas permeabilities. Moreover, these membranes can be manufactured as small-diameter (100–400 μm) hollow fibres that can provide a very large interfacial area per unit volume. Silicone membranes can be operated at high pressures without forming bubbles. However, they offer a strong resistance to mass transfer and they are much more expensive.

The majority of gas absorption experiments with microporous membranes have been performed using hydrophobic polypropylene hollow fibers. Since the pores in hydrophobic membranes stay air-filled, permeated gas is transferred by gaseous diffusion. The gas phase pressure has to be lower than that of the liquid to prevent dispersion of gas in the liquid.

The objective of this paper is to demonstrate the feasibility of water oxygenation using not hydrophobic polypropylene fibers, but hydrophilic polysulfone hollow fibers. Hydrophilic membranes are wetted by water, and oxygen is transferred through their pores by diffusion in the liquid phase, which is much slower than gaseous diffusion. The gaseous phase pressure has to be higher than the liquid pressure to prevent the latter from dispersing in the gas. A newly developed frame-type transverse flow hollow fiber module was used as a gas–liquid contacting device [21], [22]. In transverse flow hollow fiber modules, the mass transfer coefficient at the shell side is much higher than that in parallel flow modules owing to the fact that the shell-side fluid flow is perpendicular to the fiber axis. The application of transverse flow in hollow fiber membrane modules is described and investigated by several authors [2], [20], [23]–[26].

2. EXPERIMENTAL

The experiments are performed in a laboratory-made transverse flow module consisting of one 16 mm thick square submodule of plexiglass, 190×190 mm in cross-section, and two end plates of the same dimensions equipped with tube connections of 5.5 mm inside diameters (figure 1). The submodule and end plates with sealings between them were clamped together by means of twelve screws of 8 mm diameters. The submodule is composed of an internal frame, densely filled with 1058 polysulfone hollow fibers which are embedded at both their ends in the resin masses, and an external frame containing four headers for the introduction or withdrawal of fluid flowing inside the hollow fibers. The fibers are arranged in 10 parallel sheets with an effective length of 14 cm, placed alternatively in two directions at right angles. This module is designed to be a three-phase permeator, such as hollow fiber contained liquid membrane permeator [27], two-membrane permeator [28], and internally staged hollow-fiber permeator [29]. However, in this case only a two-phase contact is required, therefore two sets of hollow fibers are connected in series making a single flow line.

The fibers used for experiments are produced by X-Flow (Almelo, The Netherlands) with an inside diameter of 600 μm, a pore size of 0.2 μm, and a wall thickness of 50 μm. The hydraulic resistance of the membrane determined from the distilled water permeabilty data is $3.80 \cdot 10^{11}$ m^{-1}. The interfacial areas in this contactor equal 0.279 and 0.326 m^2 for water flow outside and inside the fibers, respectively. In order to increase the interfacial area, a number of submodules may be stacked on top of each other as shown in figure 2.

The experimental set-up employed for the investigation of membrane-based aeration of water is shown in figure 3. The feed water at 291 K containing 8–9 $mg \cdot dm^{-3}$

dissolved oxygen was pumped from a reservoir by a DCL metering pump at a flow rate of 0.3–3 $dm^3 \cdot h^{-1}$. The water flowed either through the shell side or through the tube side of the module. The pure oxygen supplied from a gas cylinder at a flow

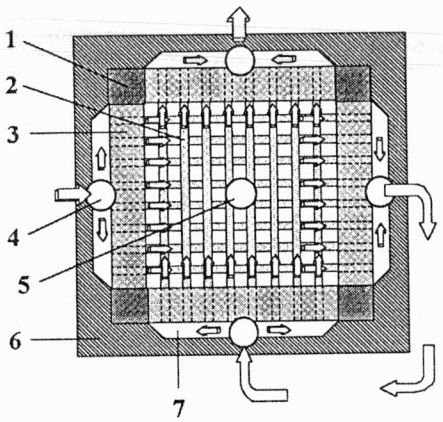

Fig. 1. Schematic view of the submodule used: *1* – internal frame, *2* – hollow fibers, *3* – resin masses (solidified glue), *4* – tube connections for fluid flowing inside the fibers, *5* – tube connections for fluid flowing outside the fibers, *6* – external frame, *7* – headers for introduction and withdrawal of fluid flowing inside the fibers

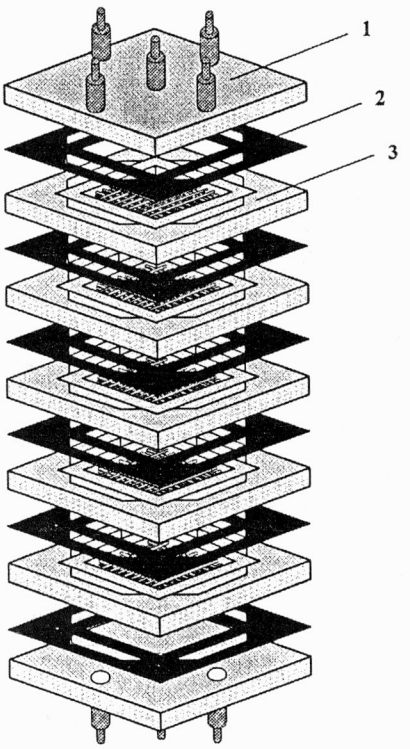

Fig. 2. Schematic view of a complete module composed of five submodules: *1* – end plates with tube connections, *2* – gaskets, *3* – submodules

rate of 20–60 $dm^3 \cdot h^{-1}$ flowed at the other side of the membrane and then was vented off to the atmosphere. The back-pressure valve was used to ensure the gauge pressure

of 2–4 kPa at the outlet gas stream, thus preventing water from dispersing as drops in the gas. The trap was located after the module captured water, which appeared due to fiber leakage at the beginning of each run. The gauge pressure in the gas stream was measured by a simple manometer filled with water. The gas flow rate was controlled by a rotameter and a wet gasmeter. The dissolved oxygen concentrations in the inlet and outlet water streams were measured by an INGOLD model 180 oxygen-sensitive electrode. After each flow rate change, sufficient time was allowed for the system to attain a steady state before another measurement was made.

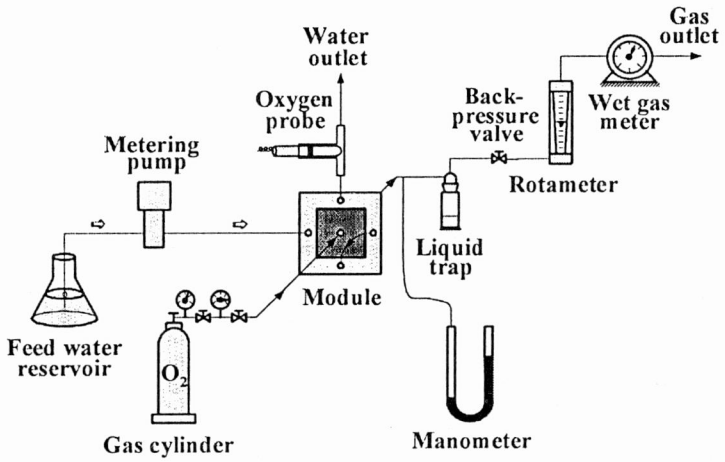

Fig. 3. Schematic view of the experimental set-up used in this work

The dissolved oxygen concentration in the outlet water stream ranged from 23.8 to 42.0 mg·dm^{-3}, depending on the water flow rate. It was used to calculate the overall mass transfer coefficient in the liquid phase K_L according to the following equation:

$$K_L = \frac{Q_L}{A} \ln \frac{C^* - C_0}{C^* - C_1}, \tag{1}$$

where C_0 and C_1 are the dissolved oxygen concentrations in the inlet and outlet water streams, respectively, C^* is the solubility of pure oxygen in water (in our experimental conditions C^* = 44.4 mg·dm^{-3}), Q_L is the volumetric flow rate of water, and A is the interfacial area. The derivation of eqn. (1) is given in the Appendix.

The overall mass transfer resistance $1/K_L$ across hydrophilic membranes is given by:

$$\frac{1}{K_L} = \frac{1}{k_L} + \frac{1}{k_M} + \frac{1}{k_G H}, \tag{2}$$

where k_L, k_M and k_G are the individual mass transfer coefficients for the liquid, membrane and geseous phase, respectively, and H is Henry's law constant.

3. RESULTS AND DISCUSSION

The overall mass transfer coefficients K_L for different locations of water in the module are given in figure 4. It is seen that K_L increases with increasing the water flow rate, the effect being more pronounced in the region of lower water flow rates. At the same water flow rate, the values K_L are much higher for water flow inside the fibers than those for water flow outside, which can be attributed to a much lower average velocity of water flowing through the shell.

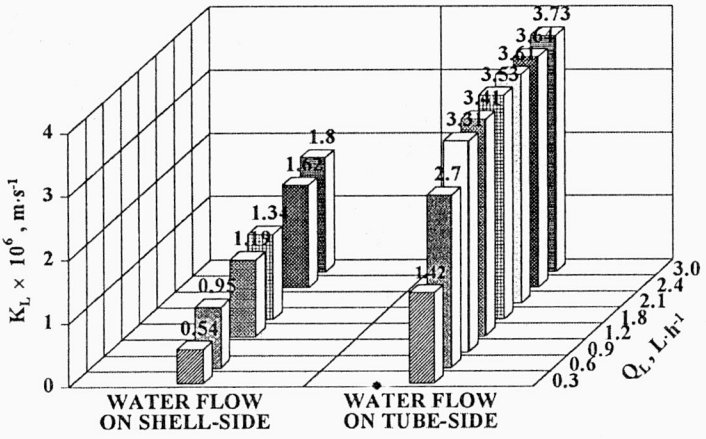

Fig. 4. Overall mass transfer coefficient versus water flow rate

In figures 5 and 6, the values K_L expressed in terms of the Sherwood number (Sh) were plotted versus the water flow rates in terms of the Reynolds numbers (Re) on a log–log scale. When water flows outside the fibers (figure 5) the Sherwood number can be expressed as [20]:

$$Sh = \frac{K_L d_o}{D}, \tag{3}$$

where D is the oxygen diffusivity in water ($D = 2.012 \cdot 10^{-9}$ m^2·s^{-1} at 291 K), and d_o is the outside diameter of the fibers. For the water flow outside the fibers the Reynolds number was calculated using the average velocity of water flowing through the shell module V_L:

$$Re = \frac{v_L d_o \rho}{\mu} = \frac{Q_L d_o \rho}{z^2 (1 - \phi) \mu}, \tag{4}$$

where $\rho = 998.6$ kg·m^{-3} and $\mu = 1.056 \cdot 10^{-3}$ Pa·s are the density and dynamic viscosity of the water at 291 K, respectively, $\phi = 0.29$ is the packing density of the fibers, and $z = 0.14$ m is the effective length of the fibers. It must be noted here that the cross-

sectional area available for flow outside the fibers varies continuously (from $z(z - n_1 d_o)$ in a plane across the fiber axes to z^2) between successive fiber sheets. A least-squares regression of the data in figure 5 gave:

$$Sh = 2.91 Re^{0.50}. \tag{5}$$

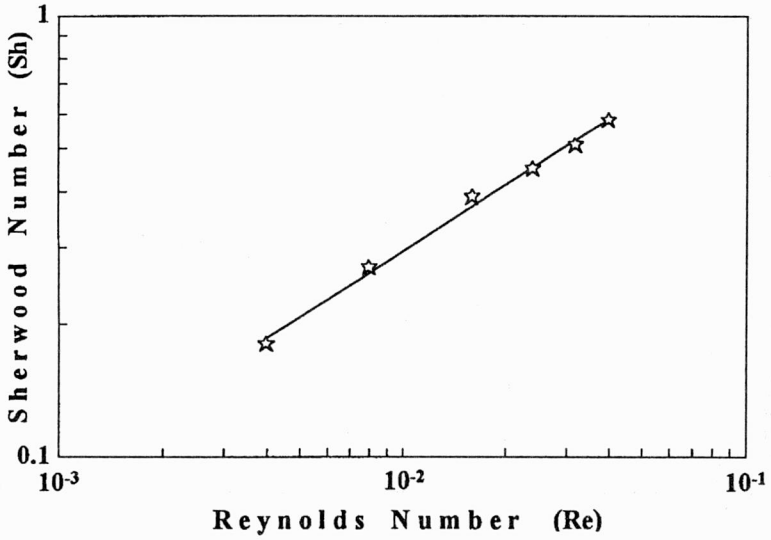

Fig. 5. The Sherwood number versus the Reynolds number for water flow outside the fibers

In this study, the effect of Schmidt number (Sc) on the mass transfer coefficient was not evaluated, so a 1/3 power dependence widely accepted in literature [3]–[33] will be incorporated into eqn. (5). The Schmidt number for a O_2–H_2O system at 291 K equals $Sc = \mu/(\rho D) = 1.056 \cdot 10^{-3}/(998.6 \cdot 2.012 \cdot 10^{-9}) = 525$, hence the corrected correlation is:

$$Sh = 0.368 Re^{0.50} Sc^{0.33}. \tag{6}$$

Therefore, for the range of water flow rates examined, the shell-side Sherwood number is proportional to the square root of the Reynolds number, which is consistent with entry region conditions anticipated in the Gröber equation [34]. The exponent of Re of 0.50 is very similar to 0.53 found by COSTELLO et al. [32] for the deoxygenation of water flowing through the shell in parallel flow hollow fiber modules of varying fiber packing density (32–76%).

Figure 6 is a plot of the Sherwood number versus the Reynolds number for the water flow inside fibers. In that case, a linear dependence of Sh on Re was only obtained at water flow rates lower than 1 $dm^3 \cdot h^{-1}$. At higher water flow rates Sh increases more slowly and approaches a constant value at high Re values. It follows from eqn. (2) that $1/K_L \to 1/k_M$ when $Q_L \to \infty$, since the gaseous phase resistance un-

der our operating conditions is negligible, i.e. $1/(k_G H) \approx 0$, and $1/k_L \to 0$ when $Q_L \to \infty$. Therefore, a limiting *Sh* value corresponds to the flow conditions under which the overall mass transfer resistance is reduced to the membrane resistance $1/k_M$.

In order to determine the membrane mass transfer coefficient k_M, the quantity $1/K_L$ is plotted versus $1/Q_L$ in figure 7 (the "Wilson plot"). A least-squares regression analy-

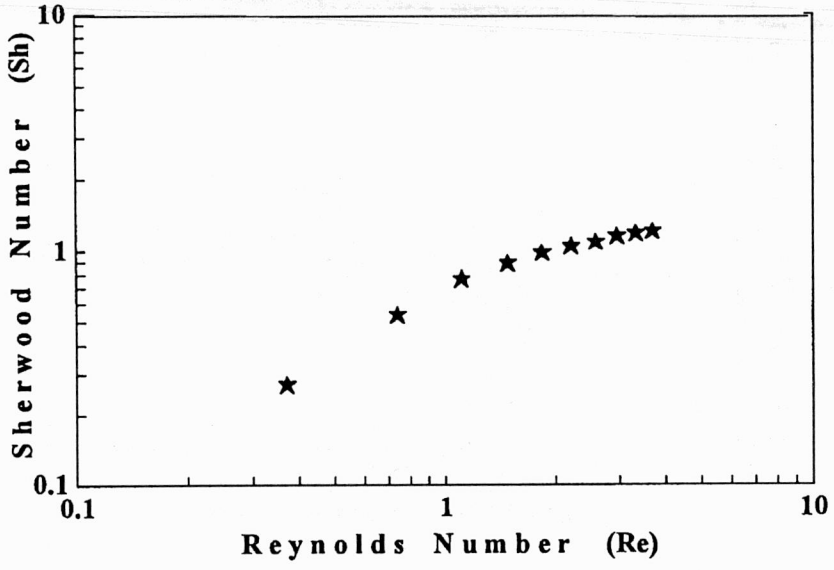

Fig. 6. The Sherwood number versus the Reynolds number for water flow inside the fibers

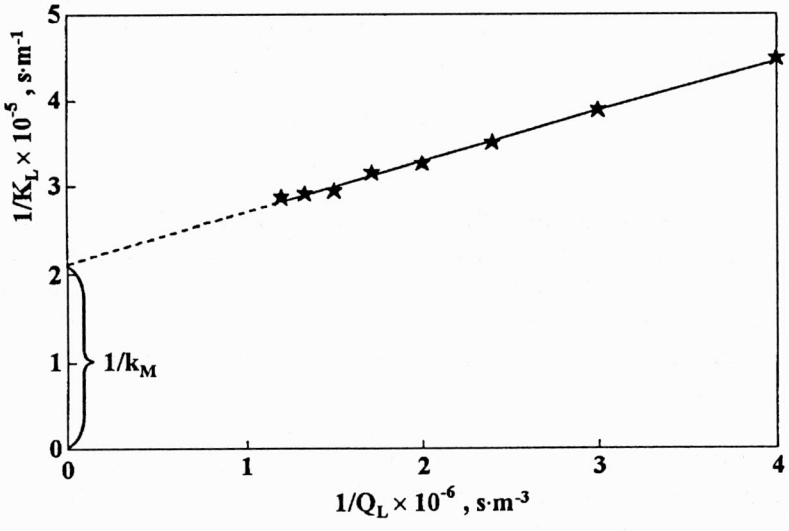

Fig. 7. The "Wilson plot" for water flow inside the fibers

sis of the data in this plot gave an intercept value of $1/k_M = 2.12 \cdot 10^5$ s·m^{-1}, from which $k_M = 4.7 \cdot 10^{-6}$ s·m^{-1}. A linear relation between $1/K_L$ and $1/Q_L$ was also observed by COONEY and JACKSON [35] for the sulfur dioxide absorption in water and by GHOST et al. [36] for the carbon monoxide absorption in cuprous chloride solution.

The value k_M of $4.7 \cdot 10^{-6}$ m·s^{-1} is three orders of magnitude lower than $5.2 \cdot 10^{-3}$ m·s^{-1} obtained by GHOSH et al. [36] for the absorption of carbon monoxide in ammoniacal cuprous chloride solution using microporous polypropylene hollow fibres. Owing to its hydrophobic nature, this membrane is not wetted by the adsorbent liquid and the pores are filled with gas. The diffusivity of carbon monoxide in the gaseous phase at 279 K is $4.59 \cdot 10^{-6}$ m^2·s^{-1} [36], which is three orders of magnitude lower than the oxygen diffusivity in water. The membrane mass transfer coefficient depends on the diffusivity D of the gas absorbed in the pores and the porosity ε, thickness δ, and tortuosity τ of the membrane wall according to $k_M = D\varepsilon/(\delta\tau)$. Accordingly, k_M is directly proportional to D and the discrepancies in k_M for polypropylene and polysulfone fibers can be explained by the differences in the values D for gas-filled and liquid-filled pores. Adopting the value τ of 3.3 for liquid-filled pores [37] and taking $\varepsilon = 0.38$, $\delta = 50$ μm, and $D = 2.012 \cdot 10^{-9}$ m^2·s^{-1} one obtains $k_M = 4.6 \cdot 10^{-6}$ m·s^{-1}, which is in a good agreement with the value k_M deduced from experimental data.

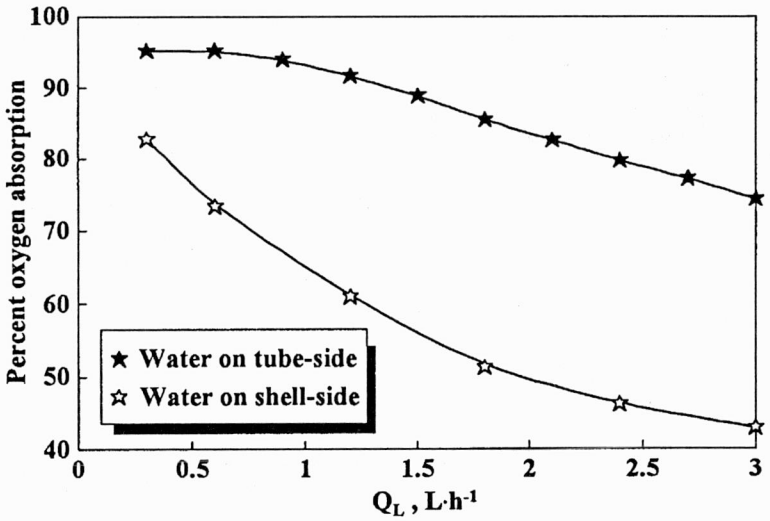

Fig. 8. The effect of water flow rate on percent oxygen absorption

The percent oxygen absorption as a function of water flow rate for different locations of liquid stream is shown in figure 8. It is seen that at the water flow rate range of 0.3–3 dm^3·h^{-1} the oxygen absorption is in the range of 74–95% and 43–83% for water flow inside and outside the fibers, respectively. As the water flow rate increases, the residence time of the water in the contactor decreases, allowing less time

for the mass transfer to occur and therefore, the percent oxygen absorption decreases. The oxygen absorption is much lower for the water flow outside the fibers, which can be attributed to a significant channelling of the liquid stream at the shell-side. The same effect was observed by COONEY and JACKSON [35] who investigated the sulfur dioxide removal from air using aqueous ammonium hydroxide solution as the scrubbing liquid in an unbaffled cylindrical module. They assumed that a substantial fraction of the fluid in the shell side flowed along the outside of the tube bundle, and not within the tube bundle.

The oxygen flux through the interfacial area J can be expressed as:

$$J = K_L \Delta C_m = \frac{Q_L(C_1 - C_0)}{A}, \tag{7}$$

where ΔC_m is the mean driving force for the oxygen transfer.

Insertion of K_L from eqn. (1) into eqn. (7) and rearrangement gives:

$$\Delta C_m = \frac{C_1 - C_0}{\ln \dfrac{C^* - C_0}{C^* - C_1}}. \tag{8}$$

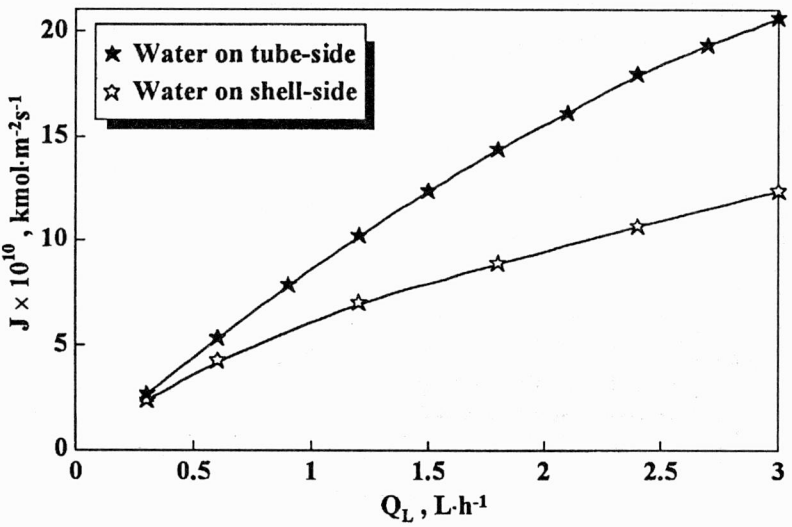

Fig. 9. The effect of water flow rate on oxygen flux through the interfacial area

As shown in figure 9, the oxygen flux through the interfacial area J increases with increasing the water flow rate due to an increase in both the mean driving force for the oxygen transfer through the membrane and the overall mass transfer coefficient. Under the same experimental conditions, the permeation oxygen fluxes are substan-

tially lower if the gas flows inside the fibers and the water flows outside. In both cases, J approaches an asymptotic value at high water flow rates, because when Q_L tends to infinity, C_1 tends to a constant value of C_0, and K_L tends to k_M. The limiting oxygen flux through the interfacial area is thus given by $J_{lim} = (C^* - C_0)k_M$. For the oxygen absorption in water containing 8–9 mg·dm^{-3} dissolved oxygen, the limiting oxygen flux through the interfacial area is in the range of $(0.9–1)\cdot10^{-9}$ kmol·m^{-2}·s^{-1}.

4. CONCLUSIONS

The dispersion-free oxygenation of distilled water by pure oxygen stream has been studied in a three-phase membrane contactor using hydrophilic polysulfone hollow fibers. The percent oxygen absorption decreases with increasing the water flow rate, while the oxygen flux through the interfacial contact area increases with the water flow rate. At a sufficiently high water flow rate, the permeation oxygen flux reaches a limiting value which corresponds to a situation where membrane wall resistance controls the overall mass transfer. The mass transfer coefficient of the membrane k_M calculated from the "Wilson plot" is $4.7\cdot10^{-6}$ m·s^{-1}, which is in a good agreement with the value calculated from the membrane wall geometry. The value k_M for hydrophilic polysulfone fibers is about three orders of magnitude lower than that for hydrophobic polypropylene fibers. It can be attributed to the fact that the pores of polypropylene hollow fibers stay air-filled, and the diffusion coefficients of gases in the air are about three orders of magnitude higher than that in the water.

REFERENCES

[1] PRASAD R., SIRKAR K.K., *Membrane-based solvent extraction*, [in:] *Membrane Handbook*, W.S.W. Ho, K.K. Sirkar (Eds.), 1992, van Nostrand Reinhold, New York, p. 727.
[2] AHMED T., SEMMENS M.J., Water Res., 1996, 30, 440.
[3] KORNFIELD J., STEPHANOPOULOS G., VOECKS G.E., Biotechnol. Prog., 1986, 2, 98.
[4] KAROOR S., SIRKAR K.K., Ind. Eng. Chem. Res., 1993, 32, 674.
[5] NII S., TAKEUCHI H., Gas. Sep. Purif., 1994, 8, 107.
[6] MATSUMOTO H., KITAMURA H., KAMATA T., NISHIKAWA N., ISHIBASHI M., Kagaku Kogaku Ronbunshu, 1992, 18, 804.
[7] MATSUMOTO H., KITAMURA H., KAMATA T., ISHIBASHI M., OTA H., AKUTSU N., J. Chem. Eng. Japan, 1995, 28, 125.
[8] NII S., TAKEUCHI H., J. Chem. Eng. Japan, 1992, 25, 67.
[9] NII S., TAKEUCHI H., Trans. Inst. Chem. Eng., Part B, 1994, 72, 21.
[10] REIJ M.W., de GOOIJER K.D., de BONT J.A., HARTMANS S., Biotechnol. Bioeng., 1995, 45, 107.
[11] ZANDER A.K., SEMMENS M.J., NARBAITZ R.M., J. Am. Water Works Assoc., 1989, 81, 76.
[12] SEMMENS M.J., REN Q., ZANDER A., J. Am. Water Works Assoc., 1989, 81, 82.
[13] SEMMENS M.J., FOSTER D.M., CUSSLER E.L., J. Membr. Sci., 1990, 51, 127.
[14] QIN R., ZANDER A.K., SEMMENS M.J., CUSSLER E.L., J. Membr. Sci., 1990, 50, 51.
[15] SU W.W., CARAM H.S., HUMPHREY A.E., Biotechnol. Prog., 1992, 8, 19.

[16] BEETON S., BELLHOUSE B.J., KNOWLES C.J., MILWARD H.R., NICHOLSON A.M., WYATT J.R., Appl. Microbiol. Biotechnol., 1994, 40, 812.
[17] TSUJI T., SUMA K., TANISHITA K., FUKUZAWA Z., KANNO M., HASEGAWA H., TAKAHASHI A., Trans. Am. Soc. Artif. Intern. Organs, 1981, 27, 280.
[18] TAI M.S.L., CHUA I., LI K., NG W., TEO W.K., J. Membr. Sci., 1994, 87, 99.
[19] YANG M.C., CUSSLER E.L., J. Membr. Sci., 1989, 42, 273.
[20] YANG M.C., CUSSLER E.L., AIChE J., 1986, 32, 1910.
[21] VLADISAVLEVIĆ G.T., MITROVIĆ M.V., 1996, Yu patent appl. No. P-39/96.
[22] VLADISAVLEVIĆ G.T., Ph. D. Thesis, 1997, The Faculty of Technology and Metallurgy, The University of Belgrade, Belgrade, Yugoslavia.
[23] FUTSELAAR H., ZOONTJES R.J.C., REITH T., RÁCZI.G., Desalination, 1993, 90, 345.
[24] BAUDET J., ROCHET M., SALMON M., VOGT B., 1976, U.S. patent No. 3, 993, 816.
[25] COUSINS R.B., 1991, European patent No. 0 419 234 A2.
[26] NICHOLS R.W., 1990, U.S. patent NO. 4, 959, 152.
[27] GUHA A.K., MAJUMDAR S., SIRKAR K.K., Ind. Eng. Chem. Res., 1992, 31, 593.
[28] SENGUPTA A., SIRKAR K.K., AIChE J., 1987, 33, 529.
[29] SIDHOUM M., MAJUMDAR S., SIRKAR K.K., AIChE J., 1989, 35, 764.
[30] DAHURON L., CUSSLER E.L., AIChE J., 1988, 34, 130.
[31] PRASAD R., SIRKAR K., AIChE J., 1988, 34, 177.
[32] COSTELLO M.J., FANE A.G., HOGAN P.A., SCHOFIELD R.W., J. Membr. Sci., 1993, 80, 1.
[33] WICKRAMASINGHIE S.R., SEMMENS M.J., CUSSLER E.L., J. Membr. Sci., 1992, 69, 235.
[34] GRÖBER H., ERK S., GRIGULL V., *Fundamentals of Heat Transfer*, 1961, McGraw-Hill, New York.
[35] COONEY D.O., JACKSON C.C., Chem. Eng. Commun., 1989, 79, 133.
[36] GHOSH A., BORTHAKUR S., DUTTA N.N., J. Membr. Sci., 1994, 96, 183.
[37] KIANI A., BHAVE R.R., SIRKAR K.K., J. Membr. Sci., 1984, 20, 125.

WYKORZYSTANIE POLISULFONOWYCH WŁÓKIEN KAPILARNYCH DO NIEDYSPERSYJNEGO (DROBNOPĘCHERZYKOWEGO) MEMBRANOWEGO NAPOWIETRZANIA WODY

Zbadano proces napowietrzania wody strumieniem czystego tlenu z wykorzystaniem niedyspersyjnych (drobnopęcherzykowych) kontaktorów membranowych z polisulfonowymi włóknami kapilarnymi. W urządzeniu utrzymywano ciśnienie 2–4 kPa, aby zapobiec przeciekaniu włókien. Stężenie tlenu rozpuszczonego w odprowadzanym strumieniu wody malało wraz ze wzrostem natężenia przepływu wody niezależnie od natężenia przepływu gazu. Dla tego samego natężenia przepływu wody stężenie tlenu rozpuszczonego w odprowadzanej wodzie jest dużo większe wtedy, gdy woda przepływa przez wnętrze włókien, niż wtedy, gdy przepływa ona na zewnątrz włókien. Całkowity współczynnik transportu masy K_L zwiększa się wraz ze wzrostem natężenia przepływu wody i osiąga stałą wartość dla dostatecznie dużego natężenia przepływu wody. W takich warunkach mikroporowate ściany membrany kontrolują całkowity transport masy.

włókno kapilarne
stężenie tlenu
napowietrzanie wody

APPENDIX

Let us consider absorption of pure oxygen by water flowing inside the hydrophilic hollow fibers in a parallel flow module (figure 10). The material balance equation of the dissolved oxygen in a module element with a length dz and an interfacial area dA is given by:

$$-Q_G dC_G = Q_L dC = K_L\left(C^* - C\right)dA, \tag{A1}$$

where Q_G is the volumetric flow rate of the gaseous phase, C_G is the oxygen concentration in the gaseous phase, and C^* is the liquid phase oxygen concentration in equilibrium with the gaseous phase.

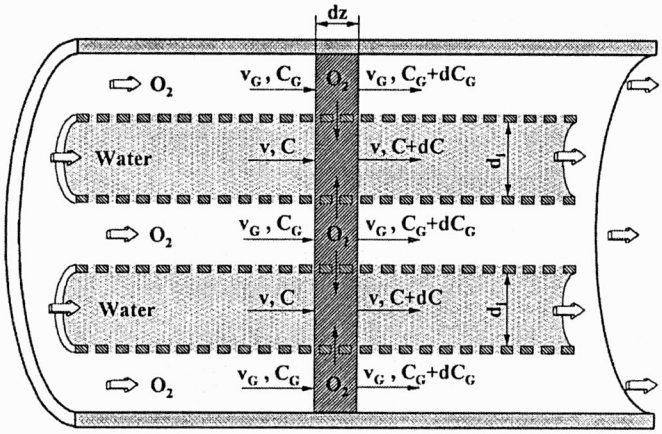

Fig. 10. Oxygen mass balance on a hollow fiber module element

According to Henry's law:

$$C_G = HC^*. \tag{A2}$$

From eqns. (A1) and (A2) the differential of the overall driving force for oxygem transfer across the membrane can be written as:

$$d\left(C^* - C\right) = dC^* - dC = -\left(1 - \frac{dC^*}{dC}\right)dC = -\left(1 + \frac{Q_L}{Q_G H}\right)dC = -H'dC, \tag{A3}$$

where H' is the Yang–Cussler dimensionless constant [30]. Inserting dC from eqn. (A3) into eqn. (A1) and rearranging yield

$$\frac{d\left(C^* - C\right)}{C^* - C} = -\frac{K_L H'}{Q_L} dA \cdot \tag{A4}$$

Integrating eqn. (A4) with the boundary conditions $A = 0$, $C^* - C = C_0^* - C_0$ and $A = A$, $C^* - C = C_1^* - C_1$ gives the following equation:

$$\ln\frac{C_1^* - C_1}{C_0^* - C_0} = -\frac{K_L H' A}{Q_L}, \tag{A5}$$

where the subscripts 0 and 1 refer to dissolved oxygen concentrations at the module inlet and outlet, respectively. For $Q_L = 3$ dm^3·h^{-1} and $Q_G = 20$ dm^3·h^{-1} one obtains:

$$H' = 1 + \frac{Q_L}{Q_G H} = 1 + \frac{3}{20 \cdot 29.79} = 1.005 \approx 1, \tag{A6}$$

where $H = 29.79$ is Henry's law constant for a oxygen–water system at 291 K and 100 kPa. Therefore, for our experimental conditions ($Q_L \leq 3$ dm^3·h^{-1}, $Q_G \geq 20$ dm^3·h^{-1}), the Yang–Cussler constant H' can be regarded as equal to unity. In addition to that, if $Q_G H >> Q_L$, the decrease in the gaseous phase oxygen

concentration over the length of the module can be neglected, so that $dC^* \approx 0$, i.e. $C_0^* = C_l^* = C^*$, and eqn. (A5) can be rearranged as eqn. (1).

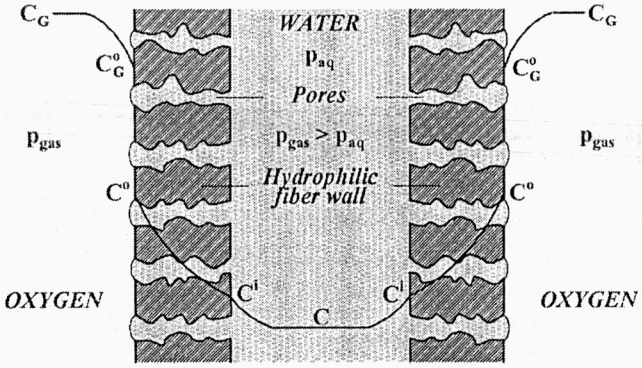

Fig. 11. Concentation profiles in gas, membrane and liquid phase for absorption of oxygen in water using hydrophilic microporous hollow fibers

The steady-state oxygen flux J across the membrane can be written with reference to figure 11 as:

$$J = K_L\left(C^* - C\right) = k_G\left(C_G - C_G^o\right) = k_M\left(C^o - C^i\right) = k_L\left(C^i - C\right), \tag{A7}$$

where the superscripts i and o refer to dissolved oxygen concentrations at the inner and outer membrane surfaces, respectively. According to Henry's law:

$$H = \frac{C_G^o}{C^o} = \frac{C_G}{C^*}. \tag{A8}$$

Recognizing that

$$C^* - C = \left(C^* - C^o\right) + \left(C^o - C^i\right) + \left(C^i - C\right) \tag{A9}$$

and applying eqns. (A7) and (A8) one can easily arrive at eqn. (2).